

Skin Allergy Detection Method using Computer Aided Design

Firas S. Abdulameer

Department of Physics College of Science, University of Mustansiriyah, Baghdad, Iraq
firasalaraji@uomustansiriyah.edu.iq

ARTICLE INFO

Received: 26 Dec 2024

Revised: 14 Feb 2025

Accepted: 22 Feb 2025

ABSTRACT

The biomedical industry is facing a major challenge in skin allergy detection and monitoring. The increasing contamination levels and consumption of unhealthy food have led to a higher number of individuals experiencing skin-related problems. As a result, the incidence of patients with skin-related issues is expanding rapidly. Nevertheless, traditional diagnostic approaches heavily rely on subjective assessments by healthcare experts, leading to inconsistencies and delays in the diagnosis process. In this work, we employed image processing and deep learning (DL) techniques to detect skin allergies in various images and evaluate the accuracy and efficiency of the methods used. The Support Vector Machine (SVM), as well as DL models including AlexNet, ResNet50, and VGG16, accomplished the detection of skin allergies in the images. A total of 2609 images, encompassing 19 different classes of skin allergy images, were utilized in this work. These images contained various types of skin allergies, such as acne, atopic dermatitis, bacterial infections, cancerous lesions, drug eruptions, eczema, lichen, melanoma, skin keratosis, and other classes. The results proved that the accuracy of the ResNet50 method was 98%, and the sensitivity value was 100% in detecting skin allergies in RGB images. From the findings, it can be said that ResNet50 outperformed the other methods employed in this work for skin allergy detection. Moreover, the accuracy and sensitivity values obtained in this work surpassed those reported in previous research studies within the same field.

Keywords: Image processing, Deep Learning (DL), Skin allergy, Image Detection, ResNet50

1. INTRODUCTION

Skin allergy, also known as allergic dermatitis or contact dermatitis, pertains to unfavorable skin reactions resulting from exposure to allergenic substances. Skin allergy is a common health issue that affects many people worldwide. Prompt and precise detection of skin allergies is essential for efficient diagnosis and treatment [1,2].

Traditional approaches to detecting skin allergies often depend on subjective evaluations by healthcare providers, leading to potential errors and delays in diagnosing the condition [3,4]. Nevertheless, recent progress in Computer-Aided Design (CAD) approaches provides encouraging possibilities for automating and enhancing the accuracy and sensitivity of skin allergy detection [5]. With the rise of CAD and machine learning, it is now possible to develop more accurate and efficient models for detecting skin allergies [6,7].

Moreover, computerized systems also utilize digital image processing (DIP) and deep learning (DL) techniques for skin allergy detection and classification in images. Skin allergies and diseases are prevalent and can affect individuals across all age groups. Given the costly nature of dermatologist consultations, there is a need for a computerized system that can evaluate patients using images of skin allergies. The images employed in this work undergo phases of DIP, including image preprocessing, feature extraction and classification, and image segmentation.

Some key features, such as shape, color, and skin lesion structures, are extracted to predict the specific classes of skin allergies and diseases [8]. In addition, CNNs are utilized for the detection of skin allergies from biomedical images. The raw dermatology images are given as input to the CNN model, and no pre-processing method is used to classify them [9].

This study aims to design a system that employs DIP and DL techniques for the detection of various skin allergies in biomedical images. In the preprocessing stage, several filters were applied to enhance the quality of the biomedical

images. In addition, these images are resized to facilitate different approaches to achieving desired outcomes. As DL techniques, AlexNet, ResNet50, and VGG16 were utilized to detect skin allergies in biomedical images. The findings from this study provided evidence that the employed methods are highly effective and accurate, surpassing the accuracy and sensitivity values reported in previous works within the field.

1. LITERATURE SURVEY

In past studies, the authors focused on skin allergy detection and classification utilizing DL techniques. In the context of skin lesion detections through DL approaches, the researchers collected different classes of images of skin allergies from local internet websites and employed data-augmentation techniques for increasing the dataset size [10].

In other research, the authors used the Xception and transfer learning DenseNet models for the detection of skin allergies. They utilized an available dataset of biomedical images in their experiments and obtained the performance scores evaluated from previous experiments of biomedical images [11]. The researchers in [12,13] investigated the detection of skin allergies and diseases by using a transfer learning model. They used a custom image dataset collected from various online sources. They used VGG16 DL and conducted a couple of separate studies.

The author Allugunti in research [14] described the proposed system to identify the skin allergies in humans using machine learning techniques. He used the K-means clustering model for segmentation, Discrete Wavelet Transform (DWT) for feature extraction, and SVM for skin allergies detection. His work aimed to classify skin allergies into four classes. In the [15], the researchers introduced an image processing approach to detect skin disorders utilizing different imaging techniques like watershed, edge detection, and morphological operations. Their method involved quantifying the number of pixels in skin lesions to analyze and extract relevant information from images. Their system was more accurate and generated results faster than traditional methods, making it an efficient system for dermatological disease detection.

The authors in [16] proposed a method to detect skin allergies and diseases utilizing DIP and DL techniques. The used ideas were simple, fast, and accurate. They detected three different types of skin allergies in their work. They used a pre-trained convolutional neural network and SVM to obtain their results.

2. MATERIALS AND METHODS

In this work, the MATLAB 2019 software is used to implement the techniques used to detect skin allergy in biomedical images and obtain the results. The process involved multiple steps, including dataset creation, preprocessing of the images within the dataset, feature extraction for both the training and validation, classification by both the SVM method and DL techniques, and skin allergy detection to achieve the desired outcomes. All steps are described in Figure 1.

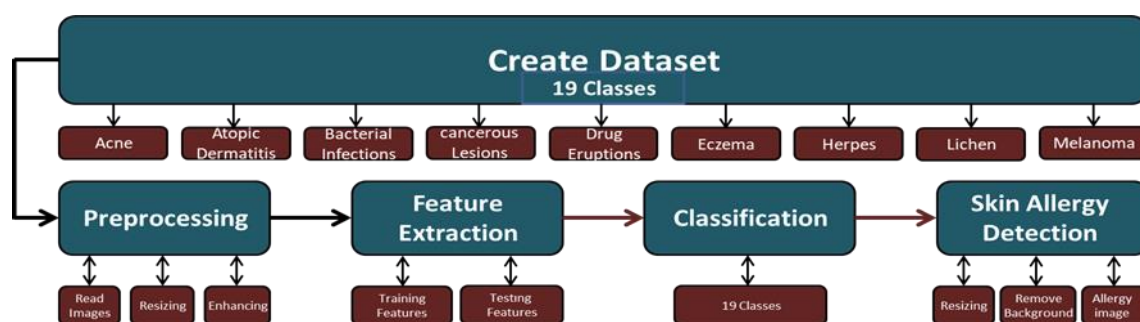


Figure 1 The proposed system Architecture.

2.1 Creation of Dataset

Availability of datasets in the dermatological world is very limited, particularly those consisting of images of skin lesions. Moreover, the current datasets that are available are often small in size and not easily accessible to the public. This can pose a significant challenge for researchers aiming to conduct reproducible studies in this area. To shed light on the current scenario, recent research has used a few dermatological image datasets. For this study, a dataset was curated in partnership with the International Skin Imaging Collaboration (ISIC), incorporating images sourced from

esteemed institutions such as Clinic de Barcelona, Medical University of Vienna, Memorial Sloan-Kettering Cancer Centre, Melanoma Institute Australia, University of Queensland, and University of Athens Medical School [17]. This database includes 2,609 images distributed in 19 different subfolders. Table 1 shows the dataset statistics used in this work.

Table 1 Dataset statistics of this work.

No.	Labels	No. of Images
1	'Acne'	840
2	'Atopic Dermatitis'	100
3	'Bacterial Infections'	65
4	'Drug Eruptions'	20
5	'Eczema'	35
6	'Herpes'	40
7	'Lichen'	62
8	'Melanoma'	24
9	'Pigmentations'	299
10	'Poison ivy'	62
11	'Ringworm'	122
12	'Skin Keratosis'	80
13	'Systemic Disease'	81
14	'Urticaria Hives'	3
15	'Vascular Tumors'	101
16	'Vasculitis Photos'	15
17	'Viral Infections'	248
18	'Wolf-Hirschhorn'	90
19	'cancerous Lesions'	322
Total		2609 images

2.2 Pre-processing Dataset

In this step, some pre-processing of the images in the dataset is done. Pre-processing include mitigating noise in the images within the dataset that might disrupt the model during training. After the noise problem, the use of dataset pre-processing becomes necessary. Another preprocessing step is to remove image background, thus isolating the objects within the image that can provide better support for the model during the classification and detection processes. The author goes on to create two distinct datasets, one containing RGB colour images and the other containing grayscale images. The last step is done to get a comprehensive understanding of the data pre-processing steps. After obtaining a maximum square image, by image resizing to 720x720 utilizing the resize function provided in MATLAB 2019 software.

Furthermore, several filters were applied to enhance the efficiency of the images within the dataset. These filters include intermediate filtering, noise removal, border cleaning, and hole-filling in objects, masking processes, and image cropping specific to skin diseases.

2.3 Dataset Images Classification

The availability of many DL models trained on datasets has made help in the subject of data detection and CAD. Furthermore, in situations where there is a scarcity of specialized labeled data, particularly in domains like

biomedical image analysis, the prevalent approach involves utilizing DL models for transfer learning [18]. This approach proves beneficial in improving performance within a limited data setting because transfer learning enables DL models trained on extensive datasets to transfer their acquired knowledge to a smaller, domain-specific dataset.

In this study, Support Vector Machine (SVM) technology was used, along with the use of three pre-trained DL models, namely VGG16, AlexNet and ResNet50 [19,20], which are well known for their effectiveness in skin allergy classification and detection. The procedures include several of the following basic steps:

2.3.1 Feature Extraction and Representation

The process of feature extraction is the output of certain layers in a neural network when certain inputs are given. The activation function in MATLAB is used to obtain the layers in a pre-trained model and thus is used to extract the features of images. In this work, a pre-trained DL model is created using three DL models: AlexNet, ResNet50, or VGG16. The resulting feature matrix will be a four-dimensional matrix, where the first three dimensions represent the size of the image and the last dimension represents the number of images. Also, a suitable name must be given to the layers whose features we need to find by using (layerName) in MATLAB. It should also be noted that this layer must be one of the available layers in the pre-trained model.

The variable (activations) in MATLAB contains the activation operations of the specific layer of the input image from the dataset to DL model. The important benefit of extracting the features of the layers is to analyse them, understand the acquired features, and use them in allergic areas in the skin and give the class name through DL. Keep in mind that different pre-trained models may have different layer names, so all layers must be reviewed to find the appropriate layer to extract the target area from the image.

2.3.2 Data Splitting

This step is one of the important steps in the DL process, as the special dataset used is separated into three important groups: training, validation, and testing. The training-set is employed to train SVM classifier and tune the DL models. The validation set helps to perform the validation process for the trained aggregates. Also, the validation set is utilized to adjust the hyperparameters and prevent over-allocation. The test-set is provided for evaluating the models performances.

2.3.3 Model Training and Hyper-parameters

To do the training, an SVM classifier was used with the features extracted from the previous stage of the training set. We tuned VGG16, AlexNet, and ResNet50 with high accuracy to get good results, using the training and validation sets. Among the adjustments that have been done to obtain good results are adjusting the learning rate, batch size, and optimization settings to get high efficiency and accuracy when classifying and detecting skin allergy regions from biomedical images.

2.3.4 Model Evaluation

We have employed some global benchmarks such as AUC, Accuracy, Sensitivity, Specificity, Precision, Recall, and G-mean to calculate the model performances. These standards employed to evaluate the trained models using the test set. The following mathematical relations are utilized in the process of finding global benchmarks for measuring performance, as follows:

Accuracy: This refers to the degree of proximity between a measurement and a predefined or accepted standard. The formula for calculating accuracy is presented in Equation (1).

$$ACC = \frac{TP+TN}{TP+TN+FP+FN} \quad (1)$$

Recall: The accuracy rate is represented here. Recall, on the other hand, assesses the inverse of certainty by comparing false negatives to true positives. Equation (2) demonstrates how to calculate recall.

$$Recall = \frac{TP}{TP+FN} \quad (2)$$

Precision: The positive analytical value demonstrates the dependability of measurements, even in cases where they deviate considerably from the accepted value. The equation for calculating precision is provided in Equation (3).

$$\text{Precision} = \frac{TP}{TP+FP} \quad (3)$$

The F1 score is utilized to strike a balance between the recall and precision metrics. Unlike the arithmetic mean, the F1-score employs the harmonic mean to calculate its value [21]. The process for computing this score is described in Equation (4).

$$F_{1(\text{Score})} = \frac{\text{Precision} \times \text{Recall}}{\text{Precision} + \text{Recall}} \quad (4)$$

2.4 Skin Allergy Detection

The proposed algorithm of skin allergy detection in this paper is depicted in Figure 2. This work aims to detect skin allergy by detecting the shape of different images in 19 classes of the dataset, and calculate its features. The region-based technique is used for skin allergy detection [22]. This method starts by obtaining images from the classification stage. The RGB images are then transformed to grayscale from [0 to 255]. These grayscale images are further transformed into binary images [0 or 1]. Subsequently, pixels in the images are grouped together to form distinct regions, each region representing a cohesive set of pixels belonging to a single object. Pixel of the image is assigned to exactly one region, denoted by its region label. Each pixel P of an image I belongs to exactly one region, specified by its region R_p , where $R_p \in \{1, \dots, K\}$. The region r is a set of pixels P_r whose $P_r = \{P : R_p = r\}$. Some regions, such as the background, do not belong to whatever object we refer to $O_r = \phi$, where O_r is the object variable. It is similar to the region where it is denoted by a set of pixels that includes the O -th objects by:

$$P_O = \bigcup_{r: O_r = O} P_r \quad (5)$$

In a similar vein, both regions and objects should consist of multiple connected components, and we ensure that no single object or region contains numerous unconnected components. The energy function incorporates the modelling of region labels, object labels, region boundary properties, and contextual relationships that establish connections between the objects and regions. We have provided a comprehensive explanation of these concepts and their integration within the energy function as follows:

$$E = \sum_r B_r^{\text{reg}} Z_r + \sum_{r,s} B_{r,s}^{\text{bdry}} + \sum_o B_o^{\text{obj}} C_o + \sum_{o,r} (C_o, Z_r) \quad (6)$$

Where B_r^{reg} is region expression, Z_r is the semantic class label, and B^{bdry} is two neighboring regions with the same appearance. This idea helps to merge the single region pixels. C_o is represented label of the related object class. B^{obj} is the boundary expression.

Once we identified the regions of the image, as mentioned earlier, we proceeded to measure various properties of these regions. These measurements included the areas of the regions, their solidity, centroids, and the pixels forming their bounding boxes. Our aim was to find the region with the highest solidity and then calculate the maximum area value under this highest solidity. This particular value corresponds to the area of the skin allergy. Moreover, we applied labeling techniques to mark both the skin allergy area and its boundaries. The area enclosed within the image boundary box represents the skin allergy features. During the final step of skin allergy detection, we took measures to visually highlight the skin allergy area. We accomplished this by surrounding it with a blue border and displaying its features, as demonstrated in Figure 2.

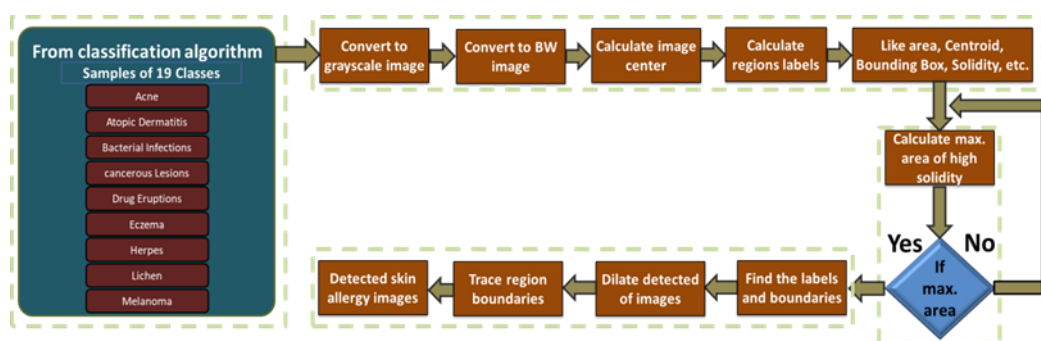


Figure 2 Skin allergy detection architecture in this work.

3. Results and Discussion

In this part, we present the results of this work, encompassing various aspects such as preprocessing, skin allergy classification, and skin allergy detection. The dataset employed in this work have 2609 images categorized into 19 classes. All the images were of size 720x720 pixels, serving as the input for the proposed algorithm.

When employing the Vgg16 technique, the image size needs to be converted from 720x720 to 224x224. On the other hand, the AlexNet technique utilizes images with a size of 227x227. Similarly, when using ResNet50, the image size must be converted to 224x224.

We studied the performance of two different experiments for skin allergy classification and detection. In the first experiment, we used a 70% for dataset as training and the remaining 30% was allocated for validation and testing purposes. In the second experiment, we used 80% of the dataset was allocated for training, while 20% was designated for validation and testing. The number of images for each experiment shows in Table 2.

Table 2 Dataset distribution according two different experiments

No	First Experiment				Second Experiment			
	Train-class	Image s-No.	Validation- and Testing	Image s-No.	Train-class	Image s-No.	Validation and Testing	Image s-No.
1	Acne	588	Acne	252	Acne	672	Acne	168
2	Atopic Dermatitis	70	Atopic Dermatitis	30	Atopic Dermatitis	80	Atopic Dermatitis	20
3	Bacterial Infections	46	Bacterial Infections	19	Bacterial Infections	52	Bacterial Infections	13
4	Drug Eruptions	14	Drug Eruptions	6	Drug Eruptions	16	Drug Eruptions	4
5	Eczema	25	Eczema	10	Eczema	28	Eczema	7
6	Herpes	28	Herpes	12	Herpes	32	Herpes	8
7	Lichen	43	Lichen	19	Lichen	50	Lichen	12
8	Melanoma	17	Melanoma	7	Melanoma	19	Melanoma	5
9	Pigmentation s	209	Pigmentati ons	90	Pigmentati ons	239	Pigmentati ons	60
10	Poison ivy	43	Poison ivy	19	Poison ivy	50	Poison ivy	12

11	Ringworm	85	Ringworm	37	Ringworm	98	Ringworm	24
12	Skin Keratosis	56	Skin Keratosis	24	Skin Keratosis	64	Skin Keratosis	16
13	Systemic Disease	57	Systemic Disease	24	Systemic Disease	65	Systemic Disease	16
14	Urticaria Hives	2	Urticaria Hives	1	Urticaria Hives	2	Urticaria Hives	1
15	Vascular Tumors	71	Vascular Tumors	30	Vascular Tumors	81	Vascular Tumors	20
16	Vasculitis Photos	11	Vasculitis Photos	4	Vasculitis Photos	12	Vasculitis Photos	3
17	Viral Infections	174	Viral Infections	74	Viral Infections	198	Viral Infections	50
18	Wolf-Hirschhorn	63	Wolf-Hirschhorn	27	Wolf-Hirschhorn	72	Wolf-Hirschhorn	18
19	cancerous Lesions	225	cancerous Lesions	97	cancerous Lesions	258	cancerous Lesions	64

In the first experiment, the size of the training feature matrix was (1827x4096), while the size of the test feature matrix was (782x4096). The number of train images was (1827x1), and the number of validation images was (782x1). For the second experiment, the size of the training feature matrix was (2088x4096), and the size of the test feature matrix was (521x4096). For the number of train images, it was equal to (2088X1), while the number of validation images was equal to (521X1).

Figure 3A depicted the Receiver Operating Characteristic (ROC) curves for the Vgg16, AlexNet, and ResNet50 techniques during the first experiment, where the dataset separated into 70% for training and 30% for validation and testing. Figure 3B depicted ROC in the second experiment. The results showed that ResNet50 technology is superior to other techniques (AlexNet and ResNet50) in terms of ROC values.

Additionally, Figure 4 showed the confusion matrices (CM) for these techniques in the same experiment. Figure 4A represented the CM for Vgg16, Figure 4B also represented the confusion matrix for AlexNet, and Figure 4C depicted the confusion matrix for ResNet50.

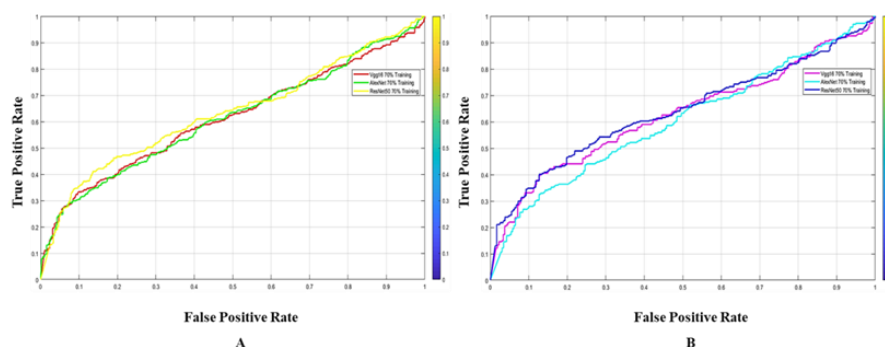


Figure 3 Shows ROC curves for the first experiment. (A) ROC curves for the Vgg16, AlexNet, and ResNet50 when training rate was 70%, validation and testing rates were 30%. (B) ROC curves for the Vgg16, AlexNet, and ResNet50 when training rate was 80%, validation and testing rates were 20%.

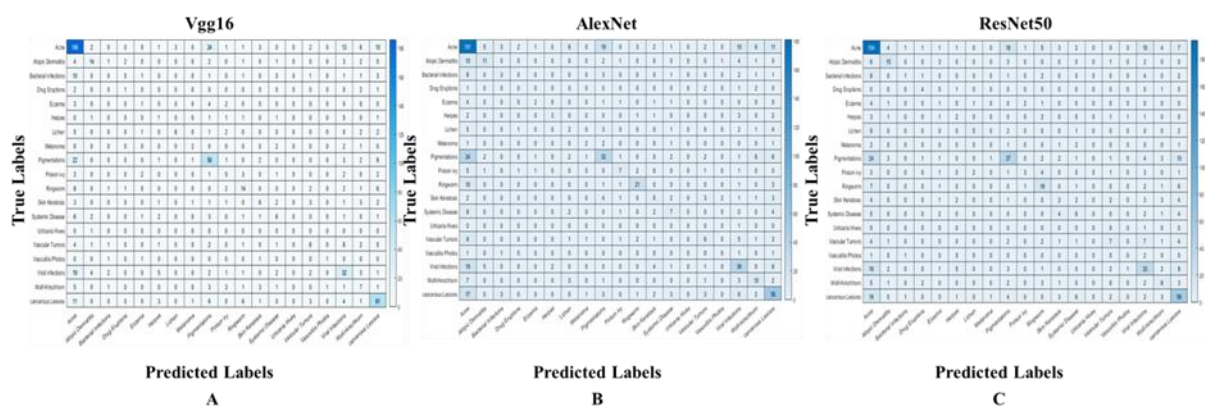


Figure 4 Confusion Matrix for the first experiment. (A) CM for Vgg16 technique. (B) CM for AlexNet technique. (C) CM for ResNet50 technique.

The figure 5 depicted the confusion matrices for Vgg16, AlexNet, and ResNet50 techniques in the second experiment. Figure 5A represented the confusion matrix for Vgg16, Figure 5B also represented the confusion matrix for AlexNet, and Figure 5C depicted the CM for ResNet50.

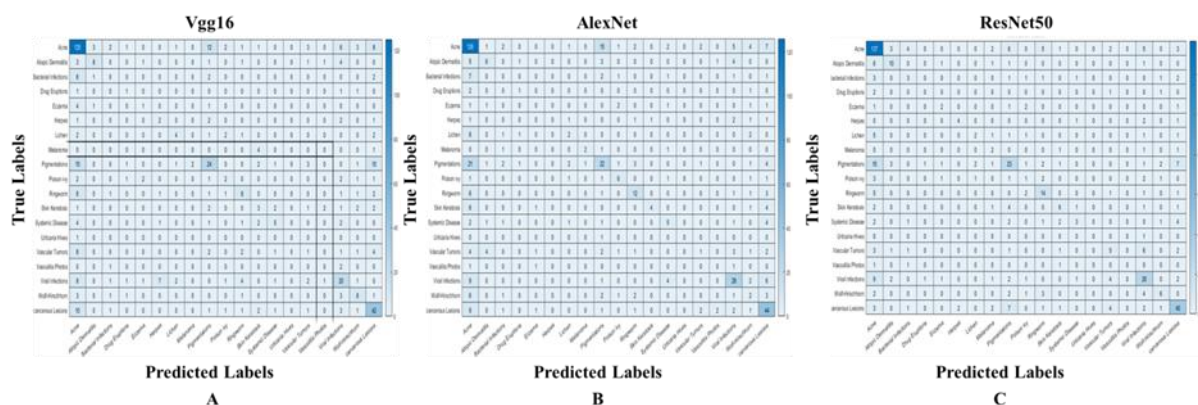


Figure 5 CM for the second experiment. (A) CM for Vgg16 technique. (B) CM for AlexNet technique. (C) CM for ResNet50 technique.

Furthermore, Table 3 provided a comprehensive performance summary, encompassing overall sensitivity (Sen.), specificity (Spec.), precision (Prec.), recall, f measurement (F-meas.), G-mean, accuracy (Acc.), and Area under ROC (AUC) values, for Vgg16, AlexNet, and ResNet50 during the first experiment. It is important to note that ResNet50 provided high accuracy (92.7%) and precision (50.8%) in classifying skin allergy images compared to other two methods (Vgg16 and AlexNet).

Table 3 Overall performance criteria of the first experiment using Vgg16, AlexNet, and ResNet50.

Experiment No: 1	Techniques	AUC	Acc.	Sen.	Spec.	Prec.	Recall	F-meas.	G-mean
	Vgg16	0.612	0.510	1	0	0.502	1	0.675	0

	AlexNet	0.611	0.83	1	0	0.491	1	0.656	0
	ResNet50	0.632	0.927	1	0	0.508	1	0.673	0

As for the performance criteria including overall sensitivity, specificity, accuracy, recall, measure f, mean g, accuracy, and area under ROC (AUC) values for Vgg16, AlexNet, and ResNet50 of the second experiment, it provided in Table 4. It is important to note that ResNet50 provided high accuracy (98.2%) and precision (54.5%) in classifying skin allergy images compared to other two methods (Vgg16 and AlexNet) in the second experiment.

Table 4 Overall performance Criteria of the second experiment using Vgg16, AlexNet, and ResNet50.

Experiment No: 2	Techniques	AUC	Acc.	Sen.	Spec.	Prec.	Recall	F-meas.	G-mean
	Vgg16	0.625	0.487	1	0	0.487	1	0.655	0
	AlexNet	0.603	0.852	1	0	0.501	1	0.667	0
	ResNet50	0.637	0.982	1	0	0.545	1	0.705	0

The results proved that the ResNet50 technique exhibited superior accuracy and efficiency compared to the other two methods in both the first and second experiments. Furthermore, when comparing the efficiency and accuracy of the ResNet50 technique between the first experiment (with a training rate of 70%, validation, and testing rates of 30%) and the second experiment (with a training rate of 80%, validation, and testing rates of 20%), it is evident that the performance of ResNet50 technique in the second experiment surpassed that of the first experiment.

Figure 6A shows images of skin allergy detection using the Vgg16 technique in the first experiment when the training rate was 70%; the validation and test rates were 30%. In contrast, Figure 6B depicted images of skin allergy detection in the second experiment, in which the training rate was 80%; the verification and testing rates were 20% using the Vgg16 technique.

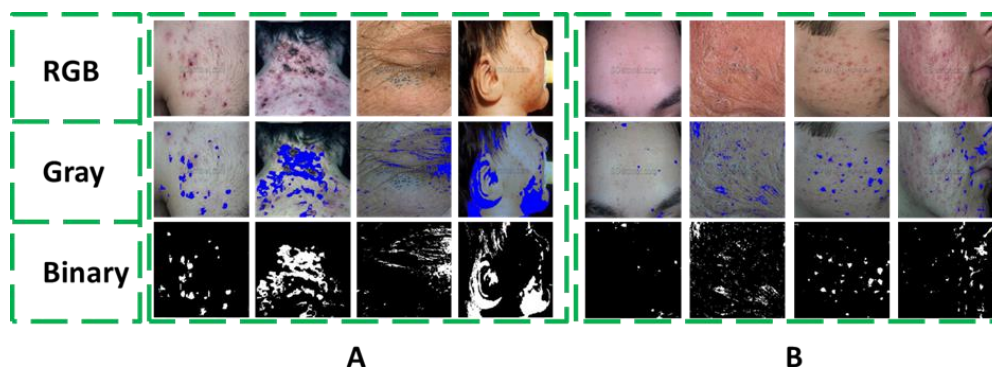


Figure 6 Detection of skin allergy in images using Vgg16 technique. (A) Detection of skin allergy at the first experiment. (B) Detection of skin allergy at the second experiment.

Similarly, Figure 7A, it is depicted the results of skin allergy detection in images using the AlexNet technique during the first experiment. On the other hand, Figure 7B employed the results of the AlexNet technique in skin allergy detection during the second experiment.

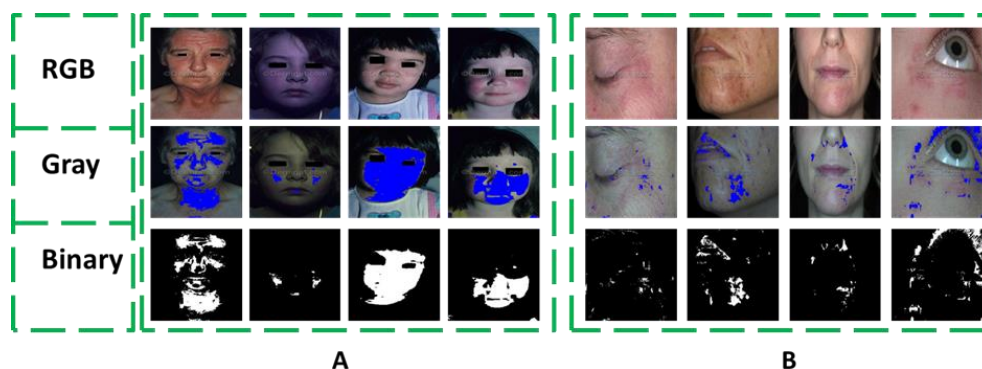


Figure 7 Detection of skin allergy in images using AlexNet technique. (A) Detection of skin allergy at the first experiment. (B) Detection of skin allergy at the second experiment.

Lastly, Figure 8A exhibits the skin allergy detection in images using the ResNet50 technique in the first experiment, with a training rate was 70%; the validation and testing rates were 30%. Furthermore, Figure 8B depicts images of skin allergy detection in the second experiment, where the training rate was 80%; the validation and testing rates were 20%, employing the ResNet50 technique.

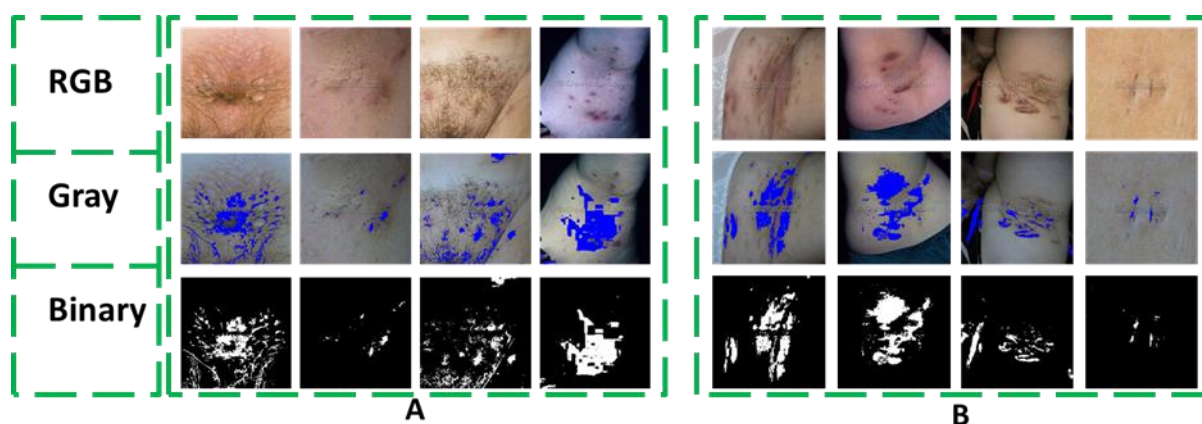


Figure 8 Detection of skin allergy in images using ResNet50 technique. (A) Detection of skin allergy at the first experiment. (B) Detection of skin allergy at the second experiment.

Moreover, it is important to mention that the approach proposed in this work to classify skin allergy in biomedical images can help us in the future when the network is updated to an advanced level from the current network, with access to more skin allergy images different from the traditional method as we do not have to retrain from scratch.

4. CONCLUSION

In this work, we proposed an architecture that used image processing and DL to classify and detect the skin allergy in biomedical images. It offers a promising approach to enhance the accuracy, objectivity, and efficiency of diagnosis. By automating the analysis of skin images and leveraging DL algorithms, these techniques provide valuable tools for healthcare professionals in identifying and classifying skin allergies.

In this study, we employed the SVM method along with three DL techniques (Vgg16, AlexNet, and ResNet50) to classify and detect skin allergy areas in images. The findings proved that ResNet50 is superior in accuracy and precision to the other used methods and techniques. The accuracy was 98.2%, sensitivity was 100%, and AUC was 63.711%. In fact, the minimum performance of all proposed networks in terms of accuracy was 48.752%.

Besides, the results proved that the proposed combined architecture presented its effectiveness and remarkable results through limited skin allergy image datasets.

Competing Interest Statement

The authors affirm that they have no known financial interests or personal relationships that could have influenced the work presented in this paper.

REFERENCES

- [1] B. O. F. Technology, Skin Disease Detection Using Image, no. 141032. 2018.
- [2] I. K. G. D. Putra, N. P. A. O. Wiastini, K. S. Wibawa, and I. M. S. Putra, "Identification of Skin Disease Using K-Means Clustering, Discrete Wavelet Transform, Color Moments and Support Vector Machine," *Int. J. Mach. Learn. Comput.*, vol. 10, no. 4, pp. 542–548, 2020, doi: 10.18178/ijmlc.2020.10.4.970.
- [3] M. Altun, H. Gürüler, O. Özkara, F. Khan, J. Khan, and Y. Lee, "Monkeypox Detection Using CNN with Transfer Learning," *Sensors*, vol. 23, no. 4, 2023, doi: 10.3390/s23041783.
- [4] I. S. S. Al Shabibi and S. Koottala, "Detection of Skin Diseases Using Matlab," *J. Student Res.*, pp. 1–10, 2020, doi: 10.47611/jsr.vi.884.
- [5] A. R. Lopez and X. Giro-i-nieto, "<EarlyUpPaleob.pdf>," pp. 49–54, 2017.
- [6] F. D. Wibowo, I. Palupi, and B. A. Wahyudi, "Image Detection for Common Human Skin Diseases in Indonesia Using CNN and Ensemble Learning Method," *J. Comput. Syst. Informatics*, vol. 3, no. 4, pp. 527–535, 2022, doi: 10.47065/josyc.v3i4.2151.
- [7] A. Shetty, K. Shah, M. Reddy, R. Sanghvi, S. Save, and Y. Patel, "Skin Cancer Detection Using Image Processing: A Review," *Lect. Notes Networks Syst.*, vol. 237, no. 6, pp. 103–121, 2022, doi: 10.1007/978-981-16-6407-6_11.
- [8] N. H. Cox and I. H. Coulson, "Diagnosis of Skin Disease," *Rook's Textb. Dermatology Eighth Ed.*, vol. 1, pp. 98–123, 2010, doi: 10.1002/9781444317633.ch5.
- [9] K. Polat and K. Onur Koc, "Detection of Skin Diseases from Dermoscopy Image Using the combination of Convolutional Neural Network and One-versus-All," *J. Artif. Intell. Syst.*, vol. 2, no. 1, pp. 80–97, 2020, doi: 10.33969/ais.2020.21006.
- [10] O. T. Jones et al., "Artificial intelligence and machine learning algorithms for early detection of skin cancer in community and primary care settings: a systematic review," *Lancet Digit. Heal.*, vol. 4, no. 6, pp. e466–e476, 2022, doi: 10.1016/S2589-7500(22)00023-1.
- [11] Nimma, D., Aarif, M., Pokhriyal, S., Murugan, R., Rao, V. S., & Bala, B. K. (2024, December). Artificial Intelligence Strategies for Optimizing Native Advertising with Deep Learning. In 2024 International Conference on Artificial Intelligence and Quantum Computation-Based Sensor Application (ICAIQSA) (pp. 1-6). IEEE.
- [12] Dash, C., Ansari, M. S. A., Kaur, C., El-Ebiary, Y. A. B., Algani, Y. M. A., & Bala, B. K. (2025, March). Cloud computing visualization for resources allocation in distribution systems. In AIP Conference Proceedings (Vol. 3137, No. 1). AIP Publishing.

- [13] Kumar, A. P., Fatma, G., Sarwar, S., & Punithaasree, K. S. (2025, January). Adaptive Learning Systems for English Language Education based on AI-Driven System. In 2025 International Conference on Intelligent Systems and Computational Networks (ICISCN) (pp. 1-5). IEEE.
- [14] Elkady, G., Sayed, A., Priya, S., Nagarjuna, B., Haralayya, B., & Aarif, M. (2024). An Empirical Investigation into the Role of Industry 4.0 Tools in Realizing Sustainable Development Goals with Reference to Fast Moving Consumer Foods Industry. In *Advanced Technologies for Realizing Sustainable Development Goals: 5G, AI, Big Data, Blockchain, and Industry 4.0 Application* (pp. 193-203). Bentham Science Publishers.
- [15] Kaur, C., Al Ansari, M. S., Rana, N., Haralayya, B., Rajkumari, Y., & Gayathri, K. C. (2024). A Study Analyzing the Major Determinants of Implementing Internet of Things (IoT) Tools in Delivering Better Healthcare Services Using Regression Analysis. In *Advanced Technologies for Realizing Sustainable Development Goals: 5G, AI, Big Data, Blockchain, and Industry 4.0 Application* (pp. 270-282). Bentham Science Publishers.
- [16] Alijoyo, F. A., Prabha, B., Aarif, M., Fatma, G., & Rao, V. S. (2024, July). Blockchain-Based Secure Data Sharing Algorithms for Cognitive Decision Management. In 2024 International Conference on Electrical, Computer and Energy Technologies (ICECET) (pp. 1-6). IEEE.
- [17] Elkady, G., Sayed, A., Mukherjee, R., Lavanya, D., Banerjee, D., & Aarif, M. (2024). A Critical Investigation into the Impact of Big Data in the Food Supply Chain for Realizing Sustainable Development Goals in Emerging Economies. In *Advanced Technologies for Realizing Sustainable Development Goals: 5G, AI, Big Data, Blockchain, and Industry 4.0 Application* (pp. 204-214). Bentham Science Publishers.
- [18] Praveena, K., Misba, M., Kaur, C., Al Ansari, M. S., Vuyuru, V. A., & Muthuperumal, S. (2024, July). Hybrid MLP-GRU Federated Learning Framework for Industrial Predictive Maintenance. In 2024 Third International Conference on Electrical, Electronics, Information and Communication Technologies (ICEEICT) (pp. 1-8). IEEE.
- [19] Orosoo, M., Rajkumari, Y., Ramesh, K., Fatma, G., Nagabhaskar, M., Gopi, A., & Rengarajan, M. (2024). Enhancing English Learning Environments Through Real-Time Emotion Detection and Sentiment Analysis. *International Journal of Advanced Computer Science & Applications*, 15(7).
- [20] Tripathi, M. A., Goswami, I., Haralayya, B., Roja, M. P., Aarif, M., & Kumar, D. (2024). The Role of Big Data Analytics as a Critical Roadmap for Realizing Green Innovation and Competitive Edge and Ecological Performance for Realizing Sustainable Goals. In *Advanced Technologies for Realizing Sustainable Development Goals: 5G, AI, Big Data, Blockchain, and Industry 4.0 Application* (pp. 260-269). Bentham Science Publishers.
- [21] Kaur, C., Al Ansari, M. S., Dwivedi, V. K., & Suganthi, D. (2024). Implementation of a Neuro-Fuzzy-Based Classifier for the Detection of Types 1 and 2 Diabetes. *Advances in Fuzzy-Based Internet of Medical Things (IoMT)*, 163-178.
- [22] Yousuf, M. M., Shaheen, N., Kheri, N. A., & Fatma, G. (2023). Exploring Effective Classroom Management Techniques in English Teaching. *International Journal on Recent and Innovation Trends in Computing and Communication*, 11(11), 382-393.
- [23] Tripathi, M. A., Singh, S. V., Rajkumari, Y., Geethanjali, N., Kumar, D., & Aarif, M. (2024). The Role of 5G in Creating Smart Cities for Achieving Sustainable Goals: Analyzing the Opportunities and Challenges through the MANOVA Approach. *Advanced Technologies for Realizing Sustainable Development Goals: 5G, AI, Big Data, Blockchain, and Industry 4.0 Application*, 77-86.
- [24] Kaur, C., Al Ansari, M. S., Dwivedi, V. K., & Suganthi, D. (2024). An Intelligent IoT-Based Healthcare System Using Fuzzy Neural Networks. *Advances in Fuzzy-Based Internet of Medical Things (IoMT)*, 121-133.
- [25] S. Inthiyaz et al., "Skin disease detection using deep learning," *Adv. Eng. Softw.*, vol. 175, p. 103361, 2023.
- [26] C. Sitaula and T. B. Shahi, "Monkeypox Virus Detection Using Pre-trained Deep Learning-based Approaches," *J. Med. Syst.*, vol. 46, no. 11, 2022, doi: 10.1007/s10916-022-01868-2.
- [27] N. S. Alkolifi Alenezi, "A Method of Skin Disease Detection Using Image Processing and Machine Learning," *Procedia Comput. Sci.*, vol. 163, pp. 85–92, 2019, doi: 10.1016/j.procs.2019.12.090.
- [28] V. R. Allugunti, "A machine learning model for skin disease classification using convolution neural network," *Int. J. Comput. Program. Database Manag.*, vol. 3, no. 1, pp. 141–147, 2022, doi: 10.33545/27076636.2022.v3.i1b.53.
- [29] P. Choudhary, J. Singhai, and J. S. Yadav, "Skin lesion detection based on deep neural networks," *Chemom. Intell. Lab. Syst.*, vol. 230, p. 104659, 2022.

- [30] B. Shetty, R. Fernandes, A. P. Rodrigues, R. Chengoden, S. Bhattacharya, and K. Lakshmana, "Skin lesion classification of dermoscopic images using machine learning and convolutional neural network," *Sci. Rep.*, vol. 12, no. 1, p. 18134, 2022.
- [31] P. Rotemberg, V., Kurtansky, N., Betz-Stablein, B., Caffery, L., Chousakos, E., Codella, N., Combalia, M., Dusza, S., Guitera, P., Gutman, D., Halpern, A., Helba, B., Kittler, H., Kose, K., Langer, S., Lioprys, K., Malvey, J., Musthaq, S., Nanda, J., Reiter, "A patient-centric dataset of images and metadata for identifying melanomas using clinical context," *Sci Data* 8, 2021. <https://doi.org/10.1038/s41597-021-00815-z>
- [32] S. J. Pan and Q. Yang, "A survey on transfer learning," *IEEE Trans. Knowl. Data Eng.*, vol. 22, no. 10, pp. 1345–1359, 2010, doi: 10.1109/TKDE.2009.191.
- [33] K. R. Avery et al., "Fatigue Behavior of Stainless Steel Sheet Specimens at Extremely High Temperatures," *SAE Int. J. Mater. Manuf.*, vol. 7, no. 3, pp. 560–566, 2014, doi: 10.4271/2014-01-0975.
- [34] Q. V. Le Mingxing Tan, "EfficientNet: Rethinking Model Scaling for Convolutional Neural Networks Mingxing," *Can. J. Emerg. Med.*, vol. 15, no. 3, p. 190, 2013.
- [35] M. Sokolova, N. Japkowicz, and S. Szpakowicz, "Beyond accuracy, F-score and ROC: A family of discriminant measures for performance evaluation," *AAAI Work. - Tech. Rep.*, vol. WS-06-06, pp. 24–29, 2006, doi: 10.1007/11941439_114.
- [36] A. Septiarini, H. Hamdani, S. U. Sari, H. R. Hatta, N. Puspitasari, and W. Hadikurniawati, "Image processing techniques for tomato segmentation applying k-means clustering and edge detection approach," in 2021 International Seminar on Machine Learning, Optimization, and Data Science (ISMODE), IEEE, 2022, pp. 92–96.
- [37] F. Garcia-Lamont, J. Cervantes, A. López, and L. Rodriguez, "Segmentation of images by color features: A survey," *Neurocomputing*, vol. 292, pp. 1–27, 2018.